Flow Model for Flooding Simulation of a Damaged Ship

Gyeong Joong Lee, *KRISO*, gjlee@kriso.re.kr

ABSTRACT

In this paper, new models for vented compartments and an accumulator model were proposed, which can adjust the inner pressure automatically, even for systems with many compartments and openings. The dynamic-orifice equation was investigated for use in the case of large openings, so that the ripples in the air pressure that had been caused by the square-root singularity of the existing orifice equation could be eliminated. In addition, some models of flow between compartments were investigated, so that the simulation could reflect more realistic situations. Application to a recent real accident validated the effectiveness of the proposed models.

Keywords: *orifice equation, flooding, air compressibility, damaged ship*

1. INTRODUCTION

While the number of flooding and sinking accidents is relatively small, they often lead to the tragic loss of personnel. Therefore, better knowledge about the processes that occur during flooding and sinking is required, and optimal response measures should be prepared according to the results of the study. For this purpose, a great deal of research about flooding has been conducted for specific real accidents, and safety assessments have been conducted during ship design, in anticipation of possible damage in the field.

The flooding simulation of a damaged ship seems to have been started by Spouge (1986), when he investigated the Ro-Ro Ferry sinking. He used a hydraulic-flow model to calculate the flood rate, and used an empirical formula to determine the center-of-gravity of the floodwater and its movement. Sen and Konstantinidis (1987) developed his method further, and they obtained the position of the center-of-gravity by assuming the free surface always remains horizontal. Later, to take into account the dynamic effect of the floodwater, Papanikolaou et al. (2000) developed the method of lumped mass. A flow equation for shallow water and the movement of point mass followed (Chang and Blume, 1998; Chang, 1999). These two papers were cited in Ruponen (2007). Computational fluid dynamics followed (van't Veer and de Kat, 2000; Woodburn et al., 2002; Cho et al., 2005); then the depth-averaged Euler equation was introduced (Lee, 2010a).

Until now, the hydraulic orifice equation has been used to obtain the flow between compartments. For the application of this equation, the following assumptions are required: incompressible fluid, inviscid fluid, steady conditions, and small openings (area). The most troublesome assumption is that steady state: the flow velocity can change instantly as the pressure changes. Lee (2014) newly derived the dynamic-orifice equation from the basic equations of fluid mechanics. In this study, the property of this dynamic-orifice equation was investigated, and the sample calculations with analysis were given.

Another problem that occurs in the simulation of ship flooding, involves the calculation of the pressure in each compartment, when many compartments are connected to each other in complicated ways. This problem has been addressed previously (van't Veer et al., 2002, 2004; Ikeda et al.,

2004; Vassalos et al., 2005). The most important thing is the determining a reference pressure for use in each compartment. Ruponen (2007) made a comprehensive study of this problem and proposed a pressure-correction method that satisfied the mass-conservation law. In this study, a new compartment model was proposed that adjusts the reference pressure simply, even for systems with many compartments and openings. And a method that takes into consideration the dynamic effect for quasi-static analysis was investigated.

2. RE-ANALYSIS OF THE ORIFICE EQUATION

In many studies, the following 'orifice equation' has been used in calculating the flow through an opening.

$$q = \rho C_D A v = \rho C_D A \sqrt{\frac{2\Delta p}{\rho}} \tag{1}$$

where, q and ρ are the mass flux and density of the flow through the opening, A is the area of the opening, Δp the pressure difference, and C_D the discharge coefficient. The above orifice equation was derived from the steady Bernoulli's equation.

2.1 Hydraulic Orifice Equation

Let us derive the hydraulic orifice equation. Bernoulli's equation can be applied to the flow of an incompressible, inviscid fluid in steady state along a stream line. Bernoulli's equation and the continuity equation used for Fig. 1 are Equations 2 and 3, respectively.

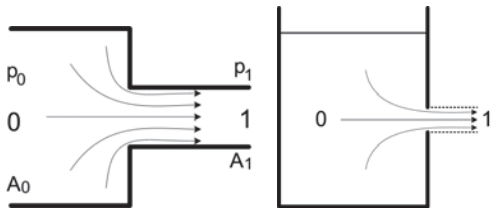

Fig. 1 Orifice and stream lines

$$\frac{p_0}{\rho} + \frac{1}{2}V_0^2 + gz_0 = \frac{p_0}{\rho} + \frac{1}{2}V_1^2 + gz_1 \tag{2}$$

$$A_0 V_0 = A_1 V_1 \tag{3}$$

where, g is the gravitational acceleration, z the height of the position, the subscripts '0' and '1' indicate the orientation (position), the fluid flows from side '0' to side '1'. The total speed of the flow is the square root of the component velocity squared, $V = \sqrt{u^2 + v^2 + w^2}$. From Equations 2 and 3, the flow velocity through the orifice can be expressed as in Equation 4.

$$V_1 = \sqrt{\frac{2}{\rho}\frac{(\Delta P + \rho g \Delta z)}{1 - (A_1/A_0)^2}} \tag{4}$$

If the area of side '0' is large, and the height difference vanishes, then Equation 4 can be reduced to the simpler form below.

$$V_1 = \sqrt{\frac{2}{\rho}\Delta p} \tag{5}$$

The flux can then be obtained by multiplying the area of orifice and fluid density.

$$q = C_D \rho A V_1 = C_D \rho A \sqrt{\frac{2\Delta p}{\rho}} \tag{6}$$

where, the discharge coefficient C_D is related to the inlet/outlet shape, and the Reynolds number. Usually for an orifice with right-angled edges, a discharge coefficient of 0.6–0.7 is used.

Equation 6 has a singular behavior of the square root function for small pressure differences. The rate of change with respect to the pressure difference, goes to infinity as the pressure difference goes to zero. Because of this, an unrealistic oscillation takes place when the pressure difference is small (as for an opening between two compartments with no

other openings), while there is no problem when the pressure difference is large. This phenomenon of square root instability is explained in detail in Appendix A. Thus, the hydraulic orifice equation (6) is for a large pressure difference, subject to the assumptions stated previously.

2.2 Dynamic Orifice Equation

There are two problems with the hydraulic orifice equation. One is that it applies to steady state conditions. The second is that it applied orifices of small cross-section (area). In order to conduct a time-domain flooding simulation, it is required to include the dynamic effect, and to expand the applicability to include orifices of large area. Let us shortly introduce the work of Lee (2014), derivation of a new dynamic orifice equation. The momentum conservation law can be represented by the Euler equation for an incompressible, inviscid fluid (Equations 7 and 7′).

$$\frac{\partial \vec{v}}{\partial t} + (\vec{v} \cdot \nabla)\vec{v} = \vec{F} - \frac{1}{\rho}\nabla p \tag{7}$$

$$\frac{\partial \vec{v}}{\partial t} + \frac{1}{2}\nabla(\vec{v} \cdot \vec{v}) = \vec{F} - \frac{1}{\rho}\nabla p \tag{7′}$$

where, $\vec{v}$ is a velocity vector, p the pressure, ρ the density of fluid, and $\vec{F}$ is the body force, including gravity. The above two equations are the same for incompressible and inviscid fluid. In this study, the integral version of the Euler equation will be used, so the momentum conservation law can be represented as in Equations 8 and 8′ for a specific control volume.

$$\int_{\Omega} \frac{\partial}{\partial t}(\rho\vec{v})dV + \int_{\partial\Omega} \rho\vec{v}(\vec{v} \cdot \vec{n})dS = \int_{\Omega} \rho\vec{F}dV - \int_{\partial\Omega} p\vec{n}dS \tag{8}$$

$$\int_{\Omega} \frac{\partial}{\partial t}(\rho\vec{v})dV + \frac{1}{2}\int_{\partial\Omega} \rho(\vec{v} \cdot \vec{v})\vec{n}dS = \int_{\Omega} \rho\vec{F}dV - \int_{\partial\Omega} p\vec{n}dS \tag{8′}$$

where, Ω is the control volume of concern, and $\partial\Omega$ is the boundary of the control volume. The orientation of the normal vector is outward normal.

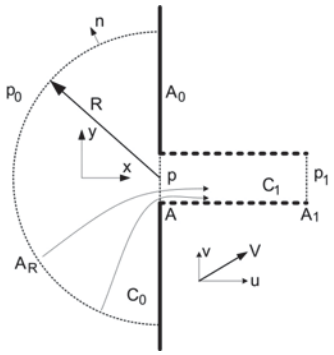

Fig. 2 Orifice, control volumes and related parameters

Fig. 2 shows the orifice and the overall shape of the control volume, where R is the distance from the center of orifice and is chosen to be large so that the flow velocity at that distance will be small enough. On the boundary, A_R, the pressure is constant as p_0, and the flow velocity is parallel to the normal vector. Let us represent the velocity vector as $\vec{v}$, the velocity normal to orifice as u, and the total velocity as $V = \sqrt{u^2 + v^2 + w^2}$, here and after. At the right side of the orifice, the velocity and pressure are assumed to be constantly distributed. The area of the orifice is $A = A_1$, the area of the wall in which the orifice exists is A_0. The control volumes on the left and right are C_0 and C_1, respectively. The velocity components, excluding u, are asymmetric about the centerline of the orifice.

Applying the mass and momentum conservation law to the control volume C_0 and C_1, we can obtain the resulting equation (9) which relates the velocity at the orifice and the pressure difference. (Lee (2014) finally got Equation 9 for the dynamic-orifice equation.)

$$\frac{\sqrt{A}}{2}\frac{\partial \bar{u}}{\partial t}+\frac{7}{8}(\bar{u})^2=\frac{(p_0-p_1)}{\rho} \tag{9}$$

where, $\bar{u}$ is the average normal velocity at the orifice. The final velocity for a steady state of the above equation is:

$$\bar{u}_f=\sqrt{\frac{8}{7}\frac{(p_0-p_1)}{\rho}} \tag{10}$$

This final steady state value is less than that provided by Equation 5. As briefly explained previously, the velocity from Equation 5 is the total velocity, and that of Equation 10 is the normal velocity at the orifice. It is reasonable to use the normal velocity for the calculation of flux through an orifice. Comparing Equations 5 and 10, it can be seen that the theoretical value of the contraction coefficient of a circular orifice with right-angle edge, is $\sqrt{4/7}\cong 0.756$ for an inviscid fluid. We can obtain the initial rate of velocity (i.e., initial acceleration) from rest using Equation 9.

$$\left.\frac{\partial \bar{u}}{\partial t}\right|_{t=0}=\frac{1}{\sqrt{A}}\frac{2(p_0-p_1)}{\rho} \tag{11}$$

The time to reach final velocity using the initial rate of change would be:

$$T=\frac{\bar{u}_f}{d\bar{u}/dt|_{t=0}}=2\sqrt{\frac{A}{7}}\sqrt{\frac{\rho}{2(p_0-p_1)}} \tag{12}$$

Fig. 3 shows the velocity rise with respect to time, when the pressure difference is a step-function.

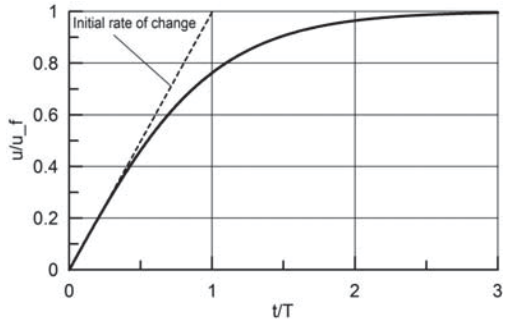

Fig. 3 Orifice velocity behavior when the pressure difference is a step function

The velocity reaches 0.765 of the final velocity at $t=T$, 0.965 at $t=2T$, and 0.99 at $t=3T$. From Fig. 3, the numerical time integration using Equation 9 seems not to be desirable if the size of time step of the simulation is less than T. For that case, one can use Equation 10 rather than 9. Here, T (from Equation 12) becomes larger as the pressure difference becomes smaller. This means that the dynamic model works for the case of small pressure differences, even if we use a fixed size of time step.

For the discharge coefficient, the use of $C_D/\sqrt{4/7}$ is desirable because of the difference between the normal velocity and total velocity in Equations 10 and 5. The density in Equation 10 should be determined according to the sign of the velocity, not the sign of the pressure difference. Equation 9 stands for positive velocity only, and we can modify the equation a little bit for both directions.

$$\begin{aligned}&\frac{\sqrt{A}}{2}\frac{\partial \bar{u}}{\partial t}+\frac{7}{8}\bar{u}|\bar{u}|=\frac{(p_0-p_1)}{\rho}\\ &\text{if } \bar{u}\geq 0, \quad \rho=\rho_0\\ &\text{if } \bar{u}<0, \quad \rho=\rho_1\end{aligned} \tag{13}$$

2.3 Large Opening

The pressure difference can vary across the orifice when it is large. If the pressure difference is constant over the orifice area, Equations 5 and 14 can give the flow velocity, but if it varies; it is possible to obtain the flow by solving the Euler equation or the Navier-Stokes equation. However, this is impractical for a system with many compartments and orifices. A more practical way is to integrate the expression over the orifice area in order to obtain the flux through the orifice. The hydraulic orifice equations (5 and 6) do not include the concept of average velocity, but for practical calculation, one can use the average concept of velocity by integrating them over

the orifice area. Meanwhile, the dynamic orifice equation (13) uses the average velocity, so it creates no logical problem to integrate the pressure difference in order to get the forces acting on the surrounding fluid. Therefore, the average velocities could be obtained using the following equations, and multiplying the orifice area gives the flux.

$$V = \frac{1}{A}\int_A \sqrt{\frac{2}{\rho}\Delta p}\, dA = \frac{1}{A}\sqrt{\frac{2}{\rho}}\int_A \sqrt{\Delta p}\, dA \qquad (14)$$

$$\frac{\sqrt{A}}{2}\frac{\partial \bar{u}}{\partial t} + \frac{7}{8}\bar{u}|\bar{u}| = \frac{1}{\rho A}\int_A \Delta p\, dA \qquad (15)$$

where, $\Delta p = p_0 - p_1$ is the pressure difference across the orifice. The mass flux can be obtained by the following equations. (The subscripts 'h' and 'd' mean the flux from the hydraulic orifice equation and dynamic orifice equation, respectively.)

$$q_h = \rho C_D A V \qquad (16)$$

$$q_d = \rho C_D{}' A \bar{u} \qquad (17)$$

where the value of C_D is from the hydraulic experiment, so use $C_D{}'$ as $C_D/\sqrt{4/7}$.

Another big problem with larger openings is the fact that the free surface may lie upon cross section of the orifice. Followings are a number of cases (Fig. 4) that could occur, depending on the height of the free surface, and the substances on both sides of the orifice.

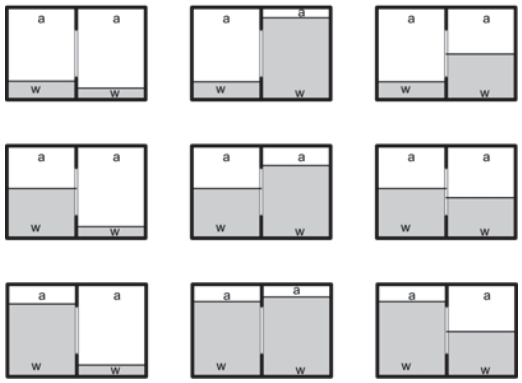

Fig. 4 Orifice and adjacent substances ('a' is air, 'w' is water)

These cases can be classified into four boundary types (within the orifice) according to the substances in contact: Air-Air, Air-Water, Water-Air, and Water-Water. The integration of Equations 14 and 15 can be obtained by dividing the orifice area into sub-regions so that each sub-region has one type of material boundary, then integrating the equations (14, 15) over each sub-region, and adding the results.

Regarding the shape of the openings, many have long, narrow shapes (e.g., doors and gaps). In these cases, one-dimensional (1-D) integration may be helpful, but for other cases the integration should be done in 2-D.

In order to calculate the flow through an opening, there is a need for several definitions. First, the identification of the compartment of interest is needed because the opening connects two compartments; thus, we have Compartment 0 and Compartment 1. This identification may be provided by adding the subscript '0' or '1'. The velocity is defined as positive when the flow is from Compartment 0 to Compartment 1; whereas, negative velocity means flow in the opposite direction. Compartment 0 is called the 'donor'; Compartment 1 is the 'acceptor'. The subscripts 'w' and 'a' refer to the substances water and air, respectively.

The two substances can flow through the opening simultaneously, so the flux may be identified by adding subscript as follows,

q_{ha} : mass flux of air using hydraulic orifice equation
q_{hw} : mass flux of water using hydraulic orifice equation
q_{da} : mass flux of air using dynamic orifice equation
q_{dw} : mass flux of water using dynamic orifice equation

First, let us divide the opening area into sub-regions with one of the four types of boundary (i.e., 'air-air', 'air-water', 'water-air', and 'water-water'). If the sign of the pressure difference changes in any sub-region, this sub-region is divided into two sub-regions so that each sub-region has a distinct sign of pressure

difference, and one boundary type. For each sub-region, calculate the following integrals,

$$I_i = \int_{A_i} sgn(\Delta p)\sqrt{|\Delta p|}\,dA \tag{18}$$

$$J_i = \int_{A_i} \Delta p\,dA \tag{19}$$

$$A_i = \int_{A_i} dA \tag{20}$$

where, $sgn(\Delta p)$ is the sign of Δp. Because the integrand has one sign, the sign of the integral is the same as the sign of the pressure difference.

The mass flux can be calculated using the above integrals, if we use the hydraulic orifice equation (21 and 22).

$$q_{ha} = \sum_i \begin{cases} \rho_{a0} C_D \sqrt{2/\rho_{a0}}\, I_i & for\ I_i \geq 0, and\ donor\ is\ air \\ \rho_{a1} C_D \sqrt{2/\rho_{a1}}\, I_i & for\ I_i < 0, and\ acceptor\ is\ air \end{cases} \tag{21}$$

$$q_{hw} = \sum_i \begin{cases} \rho_{w0} C_D \sqrt{2/\rho_{w0}}\, I_i & for\ I_i \geq 0, and\ donor\ is\ water \\ \rho_{w1} C_D \sqrt{2/\rho_{w1}}\, I_i & for\ I_i < 0, and\ acceptor\ is\ water \end{cases} \tag{22}$$

To use the dynamic orifice equation (15), the calculation should be done according to the sign of the velocity not the sign of the pressure difference. Because the velocity is the unknown, two cases (positive and negative) should be prepared. Thus,

For air-air, $J_{Pa} = \sum_i J_i\ ,\ A_{Pa} = \sum_i A_i$

$J_{Ma} = \sum_i J_i\ ,\ A_{Ma} = \sum_i A_i$

For water-water, $J_{Pw} = \sum_i J_i\ ,\ A_{Pw} = \sum_i A_i$

$J_{Mw} = \sum_i J_i\ ,\ A_{Mw} = \sum_i A_i$

For air-water, $J_{Pa} = \sum_i J_i\ ,\ A_{Pa} = \sum_i A_i$ if $J_i \geq 0$

$J_{Mw} = \sum_i J_i\ ,\ A_{Mw} = \sum_i A_i$ if $J_i < 0$

For water-air, $J_{Pw} = \sum_i J_i\ ,\ A_{Pw} = \sum_i A_i$ if $J_i \geq 0$

$J_{Ma} = \sum_i J_i\ ,\ A_{Ma} = \sum_i A_i$ if $J_i < 0$

According to the sign of the velocity, the following equations give the averaged water and air velocities.

$$\frac{\sqrt{A_{Xa}}}{2}\frac{\partial(\bar{u})_a}{\partial t} + \frac{7}{8}\bar{u}|\bar{u}|_a = \frac{1}{\rho A_{Xa}} J_{Xa} \tag{23}$$

$$\frac{\sqrt{A_{Xw}}}{2}\frac{\partial(\bar{u})_w}{\partial t} + \frac{7}{8}\bar{u}|\bar{u}|_w = \frac{1}{\rho A_{Xw}} J_{Xw} \tag{23'}$$

Equation 23 is for the air flow, and 23′ is for the water flow. In the above equation 'X' is 'P' if the velocity is positive; while 'M' is negative. The mass flux can be obtained by the following equations.

$$q_{da} = \rho_a C_D' A_a (\bar{u})_a \tag{24}$$

$$q_{dw} = \rho_w C_D' A_w (\bar{u})_w \tag{24'}$$

In some cases, the force acing on a door is required to determine when the door will collapse; the force can be obtained by simply adding all J_i.

1-D Opening

Sometimes, it is convenient to neglect the variation of the pressure difference along width and to integrate it along the height, for a door or its gap, as shown in Fig. 5.

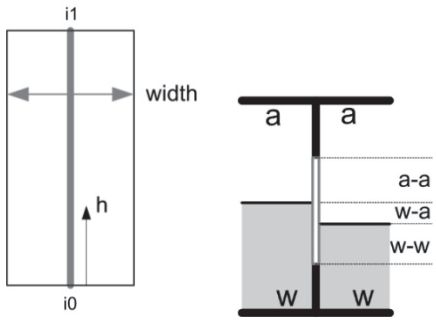

Fig. 5 Shape of 1-D opening and sub-regions of orifice

The integration of Equations (18), (19), (20) can be carried out analytically by assuming the linear variation of pressure difference in each sub-region. For the i-th sub-region, $(h_i \leq h < h_{i+1})$ the pressure difference can be represented as,

$$\Delta p = a_i(h - h_i) + b_i$$

$$b_i = \Delta p_i\ ,\ a_i = (\Delta p_{i+1} - \Delta p_i)/(h_{i+1} - h_i)$$

Then, substitute the above into Equations 18 and 19, and integrate them analytically. The results of the integrations for $a_i = 0$ are:

$$I_i = sgn(\Delta p_i) w_0 \int_{h_i}^{h_{i+1}} (|\Delta p|)^{\frac{1}{2}} dh = sgn(\Delta p_i) w_0 (|\Delta p|)^{\frac{1}{2}} (h_{i+1} - h_i) \quad (25)$$

$$J_i = w_0 \int_{h_i}^{h_{i+1}} \Delta p dh = w_0 \Delta p (h_{i+1} - h_i) \quad (26)$$

$$A_i = w_0 \int_{h_i}^{h_{i+1}} dh = w_0 (h_{i+1} - h_i) \quad (27)$$

and for $a_i \neq 0$,

$$I_i = sgn(\Delta p_i) w_0 \int_{h_i}^{h_{i+1}} (|\Delta p|)^{\frac{1}{2}} dh = sgn(\Delta p_i) w_0 \frac{2}{3a_i} \left[\Delta p (|\Delta p|)^{\frac{1}{2}} \right]_i^{i+1} \quad (28)$$

$$J_i = w_0 \int_{h_i}^{h_{i+1}} \Delta p dh = w_0 \frac{1}{2a_i} [(\Delta p)^2]_i^{i+1} \quad (29)$$

$$A_i = w_0 \int_{h_i}^{h_{i+1}} dh = w_0 (h_{i+1} - h_i) \quad (30)$$

where, $[\ ]_i^{i+1}$ means the subtraction of i indexed value from i+1 indexed value. The above expression was drawn to be independent of the sign of the pressure difference.

2-D Opening

For the general shape of an opening, the integration would be carried out in 2-D. Let us divide the opening area into sub-regions as explained previously, which can be represented as a closed polynomial. Next, integrate them over each sub-region using the Stokes theorem. Let us fit the pressure difference by bi-linear interpolation as in Equation 31.

$$\Delta p = ax + by + c \quad (31)$$

Three constants a, b, and c can be found from three conditions at three vertices of that polynomial.

Let us change the area integral to the contour integral, along the contour C_i using Stokes theorem.

$$I_i = sgn(\Delta p) \iint_{R_i} \sqrt{|\Delta p|} dx dy = \frac{2}{3a} \oint_{C_i} |\Delta p|^{2/3} dy \quad (32)$$

$$J_i = \iint_{R_i} \Delta p dx dy = \frac{1}{2a} \oint_{C_i} (\Delta p)^2 dy \quad (33)$$

$$A_i = \iint_{R_i} dx dy = \oint_{C_i} x dy \quad (34)$$

On the j-th line segment of the i-th sub-region, the following geometric relation exists.

$$x = b_{xj} y + c_{xj}, \quad b_{xj} = \frac{x_{j+1} - x_j}{y_{j+1} - y_j}, \quad c_{xj} = x_j - \frac{x_{j+1} - x_j}{y_{j+1} - y_j} y_j$$

Therefore, the pressure difference (31) can be expressed as follows on the j-th line segment.

$$\Delta p = ax + by + c = b_j' y + c_j'$$
$$b_j' = b + a b_{xj}, \ c_j' = c + a c_{xj}$$

If we integrate Equation 32, the results are (for $a \neq 0$),

$$I_i = sgn(\Delta p) \frac{2}{3a} \times \sum_j \begin{cases} \frac{2}{5b_j'} \left[(\Delta p)^2 (|\Delta p|)^{\frac{1}{2}} \right]_j^{j+1} & for\ b_j' \neq 0 \\ (\Delta p)(|\Delta p|)^{\frac{1}{2}} (y_{j+1} - y_j) & for\ b_j' = 0 \end{cases} \quad (35)$$

and for $a = 0$, $(b_j' = b, c_j' = c)$

$$I_i = sgn(\Delta p) \times \sum_j \begin{cases} \frac{2}{15b^2} \left[(5bx - 2b_{xj}\Delta p)(\Delta p)(|\Delta p|)^{\frac{1}{2}} \right]_j^{j+1} & for\ b \neq 0 \\ \frac{1}{2} (|\Delta p|)^{\frac{1}{2}} (x_{j+1} + x_j)(y_{j+1} - y_j) & for\ b = 0 \end{cases} \quad (36)$$

The results of equation (33) are (for $a \neq 0$),

$$J_i = \frac{1}{2a}\sum_j \begin{cases} \frac{1}{3b_j'}[(\Delta p)^3]_j^{j+1} & for\ b_j' \neq 0 \\ (\Delta p)^2(y_{j+1} - y_j) & for\ b_j' = 0 \end{cases} \quad (37)$$

and for $a = 0$, $(b_j' = b\ , c_j' = c)$

$$J_i = \sum_j \begin{cases} \frac{1}{6b^2}[(3bx - b_x\Delta p)(\Delta p)^2]_j^{j+1} \\ for\ b \neq 0 \\ \frac{1}{2}(\Delta p)(x_{j+1} + x_j)(y_{j+1} - y_j) \\ for\ b = 0 \end{cases} \quad (38)$$

The area, from Equation 34, can be rewritten as follows.

$$A_i = \sum_j \frac{1}{2}(x_{j+1} + x_j)(y_{j+1} - y_j) \quad (39)$$

2.4 Sample Applications

Let us consider the case in which two compartments are adjacent, and an opening is located in the wall between them. The size of the compartment is 5 m (L) x 5 m (W) x 5 m (H), and there is no vent. The sample calculations were carried out for a point and a 1-D opening, the compressibility of air was included, and an iso-thermal process was assumed. The result from the dynamic orifice equation was compared with that from the hydraulic orifice equation.

For a point opening, the area of the opening is 1 m^2 and the location of the orifice 1 m from the bottom. A 1-D calculation was also made for the comparison. The calculation cases are shown in Fig.6. The results are shown in Fig. 7 in comparison with 1-D calculation.

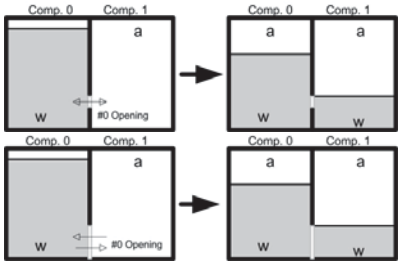

Fig. 6 Sample model for point opening (upper two) and equivalent 1-D opening (below two) (In each pair of figures, the left figure shows the initial state, and the right figure shows the expected final state.)

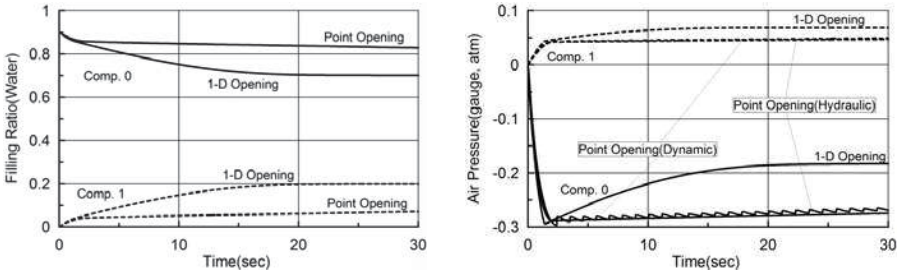

Fig.7 Filling ratio (left) and the air pressure (right) in compartments with a point-opening

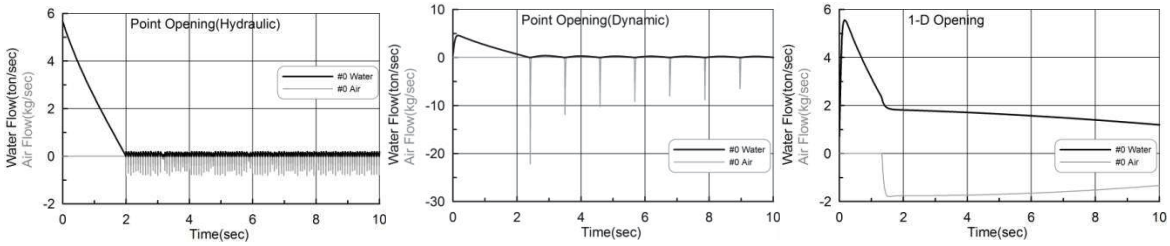

Fig. 8 Flow rates of water and air for point (left and center) and 1-D openings (right)

The filling ratio of Compartment 0 decreases with time, and the filling ratio of Compartment 1 increases. However, the results for the point-opening vary slowly, except in the initial stage, and the pressure in Compartment 0 oscillates. The flows of water and air are shown in Fig. 8.

The flow of air exhibits many rapid small oscillations with the hydraulic orifice equation, while it exhibits intermittent large oscillations with the dynamic orifice equation. This affects the pressure fluctuation in Fig. 7. This is because a point opening can only allow the flow of one substance at a time. For 1-D openings, the water and air can flow simultaneously in opposite directions, the flow is smoother, and the filling ratio reaches the value we anticipated. From these results, we now know that point-openings should not be used when there is only one opening in a compartment.

1-D opening

The next sample calculations were made with 1-D openings. The sample cases were for situations with a low opening (Case 1), a centered opening (Case 2), and two openings, one upper and one lower (Case 3). The results with a 2-D opening would be the same as the results with a 1-D opening of the same shape, if the compartments were not inclined. Here, the focus is on the comparison of the results of the hydraulic and dynamic orifice equations.

For Case 1, the model was set as in Fig. 9; the opening was located in the lower part of the wall, the height of opening was 1m and the area was $1m^2$.

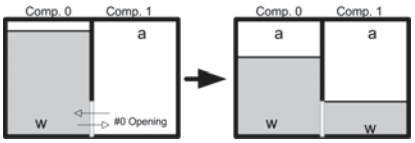

Fig. 9 Sample Case 1: low 1-D opening (The left figure shows the initial state, and the right figure shows the expected final state.)

As can be seen in Fig. 10, the calculation results for the hydraulic-orifice and dynamic-orifice equations are similar. There was no oscillation phenomenon in the results. This might be because the water totally covers the opening in the final steady stage.

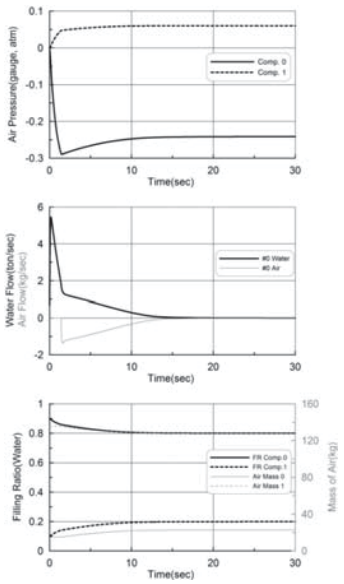

Fig. 10 Time simulation results for Sample Case 1 (low 1-D opening)

Next was Case 2, involving a 1-D opening in the middle of the wall (Fig. 11).

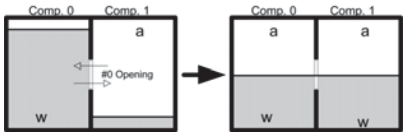

Fig. 11 Sample Case 2: centered 1-D opening (The left figure shows the initial state, and the right figure shows the expected final state.)

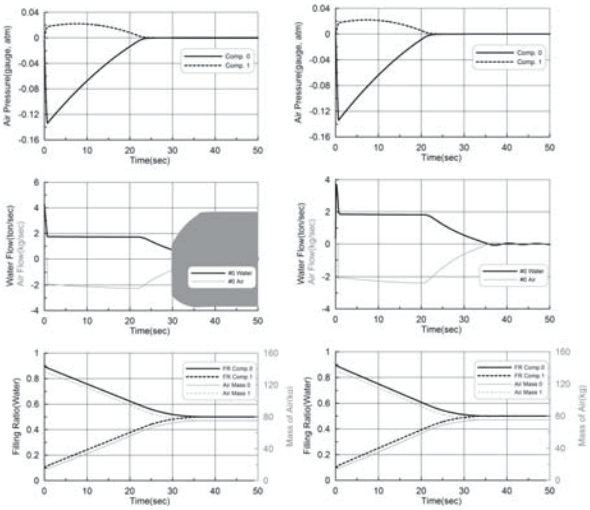

Fig. 12 Time simulation results for Sample Case 2 (centered 1-D opening), left–results from the hydraulic orifice equation, right–results from the dynamic one

The Case 2 results are shown in Fig. 12. The filling ratios are similar, but the air flows after 30 seconds are quite different from each other. The result from the hydraulic orifice equation starts to oscillate highly around 30 seconds; an enlarged view of this oscillation was drawn in Fig. 13. This oscillation is due to the numerical stability of the square root. However, the results from the dynamic orifice equation oscillated smoothly. This might be from an inertia effect.

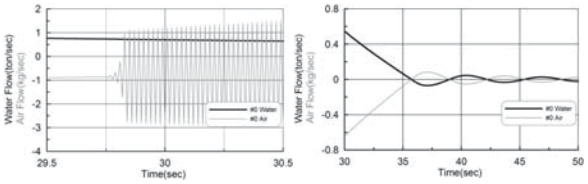

Fig. 13 Enlarged view of the flow rates of water and air: left–for hydraulic orifice equation, right–for the dynamic one)

The third sample, Case 3, involves two openings, one upper and one lower. The height of both openings is 1 m, and both openings are 1 m^2, the model was set in Fig. 14.

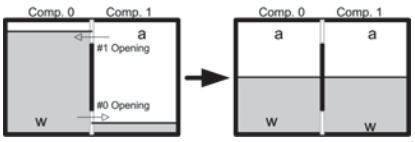

Fig. 14 Sample Case 3: two 1-D openings, one upper and one lower (The left figure shows the initial state, and the right figure shows the expected final state.)

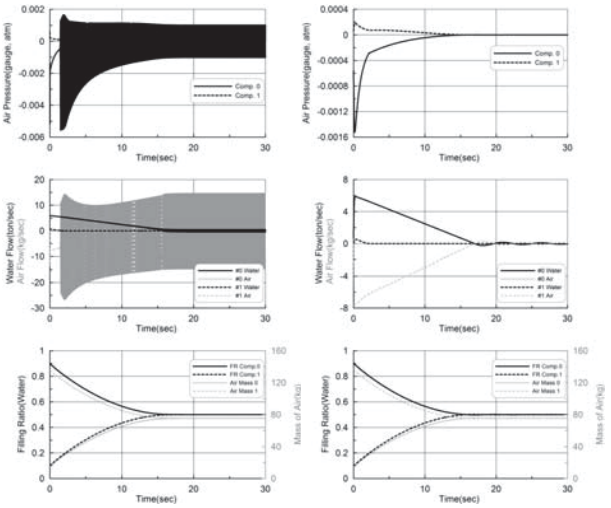

Fig. 15 Time simulation results for Sample Case 3 (two 1-D openings, one upper and one lower), left–for hydraulic orifice equation, right–for dynamic one

In this case also, the filling ratios were similar. However, the air pressure and air flow through the upper opening started to oscillate from an early stage, as in Fig. 15. Fig. 16 shows the enlarged view of the air flow and air pressure around the start of oscillation.

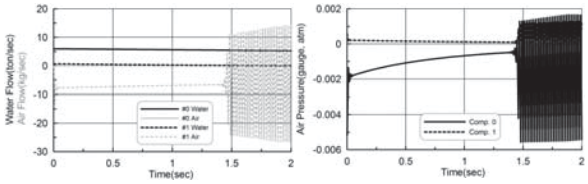

Fig. 16 Enlarged view of flow rates of water and air, and air pressure (around the starting point of the oscillation)

The results from the three sample calculations above show that the point opening should not be used for the cases with one opening in a compartment, and that the numerical instability takes place when the air in both compartments is connected through an opening. Surely, for the case of many compartments, the numerical instability due to the square-root function can ruin the flooding simulation. The dynamic orifice equation can solve this problem as it did in the above calculations.

3. COMPARTMENT MODEL

If damage occurs in a ship with many rooms, like a passenger ship, the flows of floodwater and air through the inside passages is quite complicated. The air could block the flow of water into some compartments, and retard the flooding rate. Thus, the compressibility of air plays a crucial role in the transient stage of flooding. Moreover, it is necessary to provide a reference pressure for every compartment. If a compartment is partially filled with water, the reference pressure is the one on the free surface, i.e. the air pressure. In fully water-filled compartment, there exist no free surface; so no air pressure. In such cases, selection of the reference pressure is a problem.

For a fully water-filled compartment, there is no reference pressure, while the reference pressure in a partially filled compartment is the air pressure. Ruponen (2007) introduced the idea of water height at each compartment to play the role of reference pressure in fully filled compartments. He used a method in which the pressure should be determined to satisfy the mass conservation law for each compartment, by pressure-correction. However, this method is complex and he had no choice but to use iteration to solve the pressure-correction equation

However, there is no need to focus on mass conservation. It can be satisfied automatically if we calculate the mass flux in the right way. For steady state, there is no choice but to use the iteration method to solve the non-linear pressure-correction equation. On the other hand, for unsteady problems, dynamics gives the relation between mass flow and pressure, so that the mass flow and pressure vary continuously with time, in order to maintain mass and momentum balance (i.e., via the law of conservation of mass and momentum). Therefore, if we solve the dynamic equation derived from the conservation law, the conservation will be satisfied intrinsically. The compartment that can be fully flooded is usually one with a vent. For this compartment, the mass conservation law will be satisfied if we count on the mass flowing through the air vent, that is, mass conservation for the compartment and vent, not the compartment only.

In this section, the compartment model was adapted. Then the mass of water and air, the calculation of flow in and out, and the reference pressure of the compartment, were analyzed for vented and unvented compartments.

3.1 Basic Compartment Model

Consider a compartment in which all the openings, including vents, are well defined. The mass of water and air can be calculated as,

$$\begin{aligned} \dot{m}_w &= q_w \\ \dot{m}_a &= q_a \quad (for\ m_a \geq 0) \end{aligned} \tag{40}$$

where, m_w, m_a are the mass of water and air; q_w, q_a are the mass flux of each substance into the compartment through all openings. The volume charged by water V_w is calculated by m_w/ρ_w, then the remaining volume of the compartment is the volume charged by air.

$$\begin{aligned} V_w &= m_w/\rho_w \\ V_a &= V_{max} - V_w \end{aligned} \tag{41}$$

The above equation (41) can be applied for ($V_w \leq V_{max}$) only. The state equation of ideal gas gives the pressure of the air. The state equation using pressure and density is

$$pV^\gamma = const. \quad \rightarrow \quad p/\rho^\gamma = const. \tag{42}$$

where, γ is the ratio of specific heat of ideal air, for the iso-thermal process its value is '1', and for the iso-entropic process its value is 7/5. The pressure of the air can be calculated as

$$p_a = k_{atm}\rho_a^\gamma - p_{atm} \tag{43}$$

where, the density of air $\rho_a = m_a/V_a$, and the constant coefficient of the atmospheric condition $k_{atm} = p_{atm}/\rho_{atm}^{\gamma}$. The pressure p_a is the gauge pressure, and p_{atm} is the atmospheric pressure. About the ratio of specific heat γ, the value '1' is adequate for the case that the flooding is proceeded slowly (i.e., the slow compression), and 7/5 for the case of rapid compression.

3.2 Vented Compartment Model

A vented compartment is one from which the air can flow out, if the water flows into it, without actually describing the vent duct. If the vent area (cross-section) is large enough, the pressure will remain at atmospheric. However, for a small vent area, the air would become compressed, so that the pressure of the air inside is greater than atmospheric pressure. There is no problem in calculating the flows of water and air, and the pressure, if air remains in the compartment, as in Fig. 17 (left). If, however, all the air flows out (Fig. 17, right) there is no means to calculate the pressure in it without comparing the surrounding pressure (i.e., there is no reference pressure). In this case, water can enter the compartment; the mass conservation law seems to be violated without considering the flow through the vent. If the same amount of water is understood to flow out through the vent, the mass conservation law is satisfied. We found a way to designate a reference pressure, considering the pressure at the position of the vent. For this purpose, we propose the following compartment model (Fig. 18).

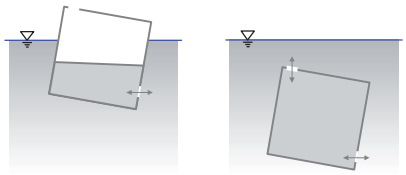

Fig. 17 Previous vented-compartment concept: floating (left) and submerged (right)

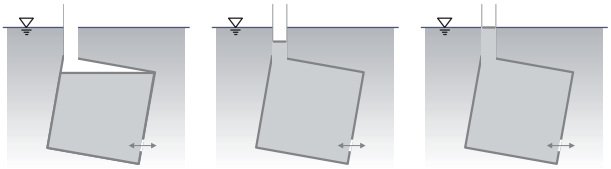

Fig. 18 Alternative air-water column concept for vented compartments

For the real vent duct (or ducts) substitute a simple vertical (virtual) vent (i.e., introduce a vertical air-water column at the top of the compartment). For the case of partial filling, there is no problem, and the reference pressure is the air pressure. Even for the case of full filling, the water can flow into the compartment; the surplus water flows up through the vertical vent. The surplus water fills the vertical vent and the top surface goes up to the free surface, and the reference pressure will be set to the pressure corresponding to the height of the water column in the vertical vent. If more water flows into it, the height of water column will be higher than the free surface, and the reference pressure will be higher than the surrounding compartment. If so, the water in that compartment could flow out to another compartment, and the water column could be reduced (that is, the reference pressure will be set to the correct value automatically as the event progresses). The above assumptions explain real situations well, and the conservation of mass is satisfied.

To continue, the compartments can then be categorized into partially vented and fully vented compartments. If the vent area is large, the air is easily vented if the water flows in, so the air pressure is almost the same as atmospheric pressure. If the vent area is small, the air will be compressed. From these, the criterion for a fully vented compartment can be drawn. It seems reasonable that a fully vented compartment has a virtual vent area greater than 1/100 of the top area. A compartment with a vent area less than 1/100 of the top area would be classified as a partially vented compartment.

Fully Vented Compartment

Let us assume the vent area $A_v = 0.01 \times (V_{max})^{2/3}$ or the area of water flow in. Then air compressibility is nearly absent. For fully vented compartments, the flow model can be described for V_w/V_{max} <1, i.e., the case in which air remains,

$$\begin{aligned} \dot{m}_w &= q_w \\ V_w &= m_w/\rho_w \\ p_a &= 0 \end{aligned} \tag{44}$$

for $V_w/V_{max} \geq 1$, i.e. fully water-filled, $(V_v \geq 0)$

$$\begin{aligned} V_w &= V_{max} \\ \dot{V}_v &= q_w/\rho_w \\ h_v &= V_v/A_v \\ p_a &= \rho_w g h_v \end{aligned} \tag{45}$$

where, h_v, V_v are the height and volume of the water column in the vertical vent, respectively.

Partially Vented Compartment

In this model, the air pressure is sought. Suppose that A_v is given.

For V_w/V_{max}<1,

$$\begin{aligned} q_{av} &= \begin{cases} C_D \rho_a A_v \sqrt{2p_a/\rho_a} & for\ p_a \geq 0 \\ -C_D \rho_{atm} A_v \sqrt{-2p_a/\rho_{atm}} & for\ p_a < 0 \end{cases} \\ \dot{m}_w &= q_w \\ \dot{m}_a &= q_a + q_{av} \\ V_w &= m_w/\rho_w \\ V_a &= V_{max} - V_w \\ \rho_a &= m_a/V_a \\ p_a &= k_{atm}\rho_a - p_{atm} \end{aligned} \tag{46}$$

For $V_w/V_{max} \geq 1$, i.e. fully filled, $(V_v \geq 0)$

$$\begin{aligned} V_w &= V_{max} \\ \dot{V}_v &= q_w/\rho_w \\ h_v &= V_v/A_v \end{aligned} \tag{47}$$

$$p_a = \rho_w g h_v + p_{vent}$$

where, in the last equation p_{vent} is the pressure loss due to the flow through the vent. It can be represented by the equation $p_{vent} = 1/2\ \rho\ v^2$, in which the velocity and density is assumed to be those of the air flowing through the vent.

When the filling ratio (V_w/V_{max}) reaches '1' (i.e., the substance that flows through the inlet of the vent changes from air the water), the volume of the air (V_a) vanishes. So, we have trouble in calculating the density of air. To remedy this, it is required to add the volume of the vent to V_a, and the mass of air in the vent to the air mass of the compartment. At the moment when the compartment is just fully filled, the pressure of air (i.e., the reference pressure) has a jump to p_{vent}. If we use the density and velocity of the water, this gives very large value at that moment, whereas it will soon be balanced with the adjacent compartment. So it is recommended to use the density and velocity of the air through the vent, and add some damping to it.

3.3 Accumulator Model

If a compartment is not vented, usually all the air does not flow out. Of course, all the air could flow out if there were any openings at the top of the compartment. If air remains in the compartment, the air pressure can be calculated using the state equation of air (Equation 43). On the other hand, if the amount of air is very small, the air pressure is so largely affected by the amount of water inflow, that it is difficult to calculate the air pressure. Furthermore, if all the air flows through an opening, there is no means to calculate the air density, thus a problem arises in calculating the reference pressure. In fact, a compartment in a ship might have machinery, freight, and many other things in it, so that there might be many small spaces that could contain air. This means that all the air in a compartment seldom flows out. Let us

introduce a virtual accumulator that could solve this problem.

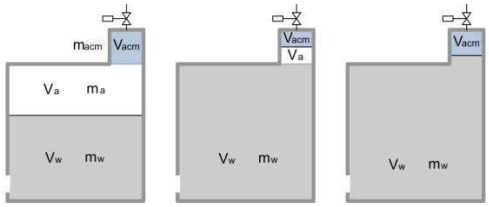

Fig. 19 Virtual Accumulator Model

Fig. 19 shows the concept of a virtual accumulator for several cases: a case with remaining air, a case with a very small amount of remaining air, and a case without air. Air fills the accumulator, and its maximum volume is represented as V_{acmmax}, the operating volume is V_{acm}, and the air mass in the accumulator is m_{acm}.

A simple way to apply the accumulator is by adding the extra air volume without pre-charged pressure to the compartment volume, which cannot flow out. This is a passive accumulator, and its mathematical model is Equation 48.

$$\begin{aligned}
&\dot{m}_w = q_w \\
&\dot{m}_a = q_a \ (for\ m_a \geq 0) \\
&V_w = m_w/\rho_w \\
&V_a + V_{acm} = V_{max} + V_{acmmax} - V_w \\
&\rho_a = \frac{m_a + m_{acm}}{V_a + V_{acm}} \\
&p_a = k_{atm}\rho_a - p_{atm} \\
&V_a = m_a/\rho_a \\
&V_{acm} = m_{acm}/\rho_a
\end{aligned} \tag{48}$$

The virtual accumulator has the effect of enlargement of the volume. Even when there is no air the accumulator can provide a reference pressure and stabilize pressure fluctuation. If a passive accumulator is used, the mass conservation law is violated a little. However, if we want to conserve mass strictly, the active accumulator ensures it. An active accumulator makes the accumulator volume constant by controlling the amount of air. If the water flows in, the air in the accumulator is compressed so that the reference pressure rises and blocks the inflow of water. In this way, the active accumulator can give the reference pressure and ensures the mass conservation law in that compartment. A sudden inflow violates the mass conservation law, but in a short time, the appropriate amount of water flows out, so that the inner mass of compartment remains constant in reference to the concept of time average. The active accumulator model simply adds a feedback control law to regulate the volume of the accumulator. This allows the accumulator to maintain a nearly constant volume, and this feedback control changes the mass of the accumulator as in Equation 49.

$$\begin{aligned}
&V_{in} = V_{acmmax} - V_{acm} \\
&\dot{m}_{acm} = k_P V_{in} + k_D \dot{V}_{in}
\end{aligned} \tag{49}$$

where, k_P, k_D are the proportional and differential gains respectively, V_{in} means the change of the accumulator volume from its initial one (i.e., the volume that enters the accumulator). Through many calculations, we found that 5% of the compartment volume is reasonable for a maximum accumulator volume, and $k_P = 1$, $k_D = 10$ are adequate for almost all the cases with $\Delta t = 0.01s$. For other values of Δt, the adequate values of control gains may differ, of course.

3.4 Floodwater Dynamics

In this study, the movement of the center-of-gravity was analyzed using quasi-static analysis. This analysis has no dynamics, so that the center-of-gravity moves instantly to a new position if a compartment inclines. However, in real situations, time is required for the floodwater to accumulate in new locations, and some complicated flow motions arise, typically waves. Quasi-static analysis has no dynamics effect, so it cannot reflect this reality. In flooding simulation, this effect is large for a ship like a Ro-Ro ferry, which has a large car deck. Suppose that a ship contains floodwater, even if it is inclined only a little bit, the shift in the floodwater center-of-gravity is largely

instantaneous (by previous methods). Therefore, the calculated motions of the ship include unrealistic motions because of the instant large shifts in the center-of-gravity. In this study, a simple method is proposed that considers the dynamics of the floodwater.

The center-of-gravity moves toward the geometric center as time goes, so we want a method that provides a force toward the static center-of-gravity, and that also provides adequate damping. The appropriate mathematical model for the movement of floodwater might be a second-order differential equation in the form of Equation 50.

$$m\dot{v} + bv = f \times (x_S - x) \tag{50}$$

where, x is the center-of-gravity of floodwater, while x_S is the static one; m is the mass of floodwater, and v the moving velocity of the center-of-gravity. If the static center-of-gravity does not move, the center-of-gravity moves toward the static one.

The forcing factor f seems to be proportional to the mass and gravity, and be a function of the filling ratio f_r. So, we propose the equation of motion of the center-of-gravity as follows,

$$m\dot{v} + bv = mg\frac{1+2f_r}{l/2}(x_S - x) \tag{51}$$

where, l is a characteristic length of the compartment. Dividing the above equation by the mass, the equation can be represented as a typical second-order differential equation.

$$\begin{aligned} &\ddot{x} + b'\dot{x} + \omega_n^2 x = \omega_n^2 x_S \\ &\omega_n^2 = \frac{2(1+2f_r)g}{l} \\ &b' = \omega_n \end{aligned} \tag{52}$$

Let us also consider the damping coefficient b'. If the damping is critical, it is $b'_c = 2\omega_n$. In order to reflect more realistic situations, it is better to have an overshoot, so let us take 1/2 of the critical value. If we take this value, the amplitude of RAO at resonance is '1'. The above equation shows that the center-of-gravity moves slowly if the characteristic length is long, and moves quickly if the length is short. This reflects reality. Consider the natural frequency of Equation 52. The natural frequency of the first resonance mode of a standing wave in a tank whose length is l can be found in Equation 53.

$$\begin{aligned} &\omega_n^2 = \frac{\pi g}{l} \\ &\text{from } (\tfrac{1}{2}\lambda = l, k = \frac{2\pi}{\lambda} = \frac{\pi}{l}) \end{aligned} \tag{53}$$

Comparing the two resonance frequencies (52, 53), if the filling ratio is about 0.3, the two frequencies are similar. As the filling ratio decreases, the effect of shallow water makes the natural frequency lower, and as the filling ratio increases, the natural frequency becomes higher. This characteristic is already included, approximately, in Equation 52.

The advantage of this equation is the fact that we can consider the effect of the filling ratio in a simple manner. If we can determine the static center-of-gravity, Equation 52 gives the motion of the center-of-gravity without involving complex fluid dynamics.

4. VALIDATION

Recently, there was a sinking accident with the loss of many people in Korea. The ship, MV Sewol, was a Ro-Ro ferry of 132m length, 22m breath, and 9,610ton displacement. It has two car decks and a freight deck in it. The simulation team in KRISO was launched in order to make data to reasonably explain the cause and effect of the accident (KRISO, 2014). The main reason of the accident turned out to be the lack of restoring and the movement of freight during its turn. The ship was modeled

with 27 internal compartments and 81 openings for flooding simulation. Figure 20 shows the shape of the ship and compartments in it. The flooding simulation team had tried to tune up the parameters (especially related with openings, the gap of doors and ramps) so that the simulation results resemble the official data from the cooperative investigation headquarter for MV Sewol. Then, the team provided explanations about the process of the flooding and sinking.

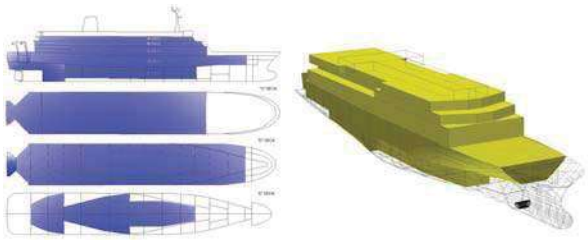

Fig. 20 Shape and the internal compartments of MV Sewol

It was presumed that the ship tumbled down due to an excessive steering and the resulting movement of freight in it. It was reported the initial angle of heel was 30 degrees port after its tumble and there was no collision accident. The flooding simulation started from the condition in which the roll angle was negative 30 degree (i.e., the left side of the ship went down). Fig. 21 shows the roll angle (inclination) compared with the official data provided by the cooperative investigation headquarter for MV Sewol. Fig. 22 shows the pitch and heave motion during flooding and sinking.

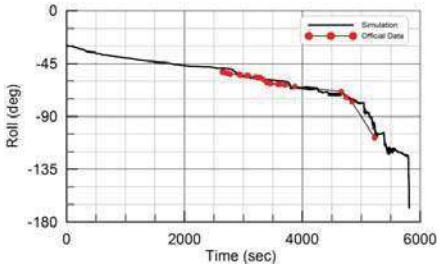

Fig. 21 Inclination angle(roll) compared with the official data

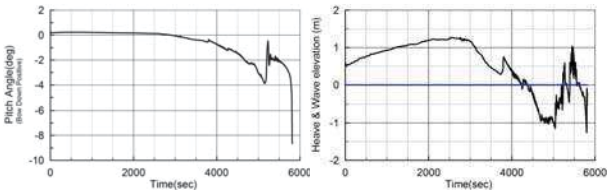

Fig. 22 Pitch(left) and heave(right)

Fig. 23 shows the flow rate through some important openings from outside. And Fig. 24 shows the filling ratios in compartments below the main deck. At the start, the flow-in took place only through the side door located at D deck. As the inclination went larger, the flow-in through the stern ramps began to grow. There were only 3 openings through which the sea water flows in before 2,700 seconds. The resulting floodwater was piled up in D deck and E deck (these decks is located under the main deck). After 2,700 seconds, the sea water flowed in through the vent of the left stabilizer room. And after, many other compartments flooded.

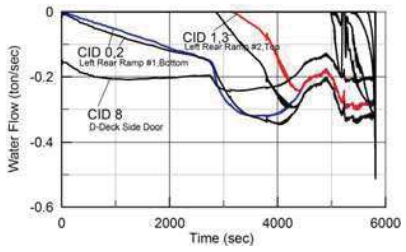

Fig. 23 Flow rate of water through important openings

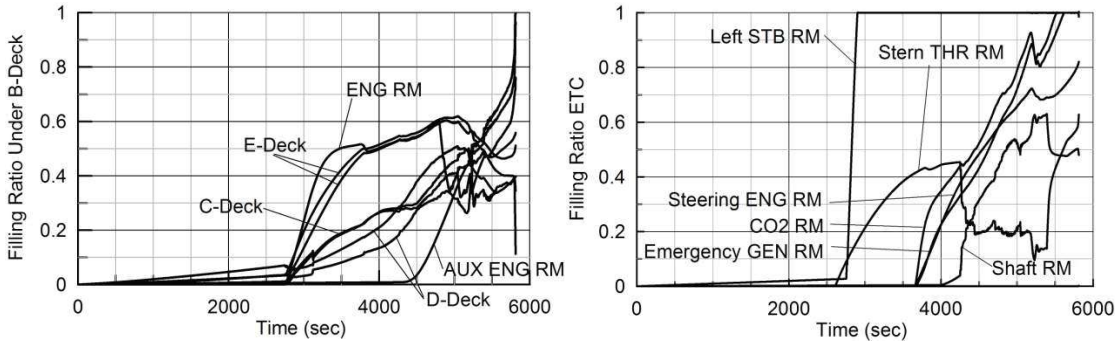

Fig. 24 Filling ratios of the lower compartments (below main deck)

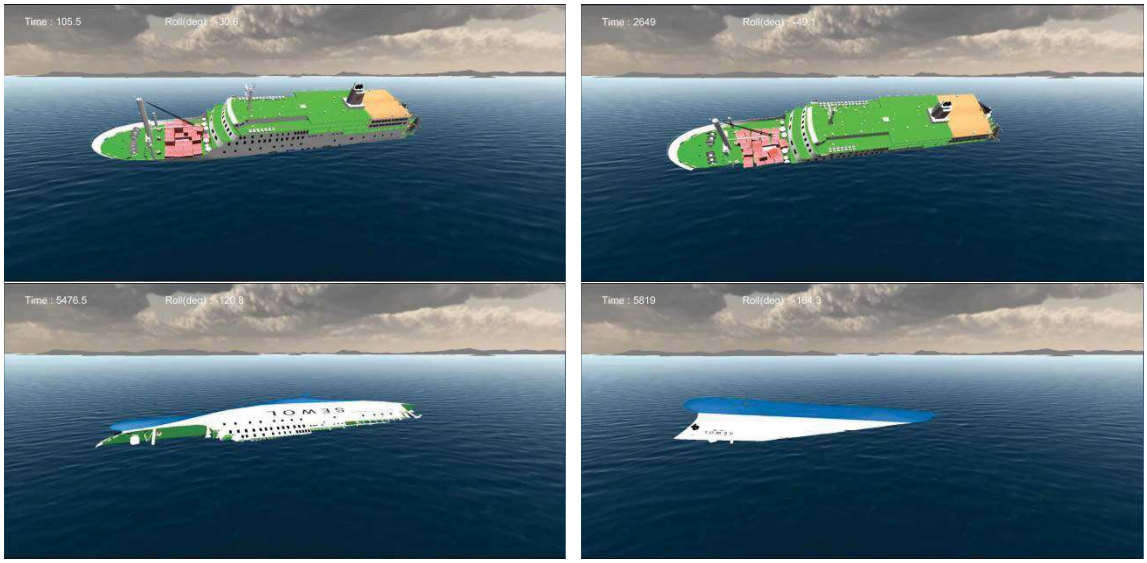

Fig. 25 Visualizations of the simulation results (upper left: initial state, upper right: when the coast guard arrived, lower left: when the last rescue action, lower right: final state)

The side door located at D deck and the rear ramps are assumed to be closed. The simulation team assumed gap of 0.01m along the edge of the door and ramps. It could be said that the only 0.01m of gap size of a side door and rear car ramp are sufficient to flooding and sinking of Ro-Ro ferry.

Fig. 25 shows the important situations to be noticed: initial condition of flooding simulation, the ship when coast guard arrived, when the last rescue action played, finally capsized. The results reflect the actual situations well, in comparison with the pictures that have shown in many mass medias.

5. CONCLUSIONS

In this study, flow models for simulation of ship flooding were investigated. The most important matters were the orifice equations and the compartment models. For the orifice equation, it was shown that numerical instability could occur involving the air flow, if the hydraulic orifice equation is used to calculate the flow through an opening. A newly derived dynamic orifice equation by Lee (2014) was investigated that could resolve the numerical instability that comes from the square root of the pressure difference. A new compartment model that can provide pressure balance automatically was proposed. It reduces the computational burden and difficulty in applying the pressure-correction method.

Furthermore, practical models indispensable for application to realistic situations were investigated. These included down flooding and a simple method for giving the dynamic effect of floodwater in quasi-static analysis.

Using these models, the flooding simulation of a recent actual accident was carried out. When the results were compared with official data, the process of the flooding and sinking could be explained approximately, but reasonably.

6. ACKNOWLEDMENTS

In the accident mentioned in this study, the ship sank with the loss of many people, dead or missing. The data included in section 5 are parts of the report of the simulation team for the accident of Ro-Ro ferry. The writer feels sorry for not adding the details of the report of the simulation team of this accident in this paper. The writer hopes that this study helps to make ships safer. This study was partially supported through a basic project of KRISO(PES1990).

7. REFERENCES

Chang, B.-C., Blume, P., 1998. "Survivability of Damaged Ro-Ro Passenger Vessels", Schiffstechnik – Ship Technology Research, Vol. 45, pp. 105-112.

Chang, B.-C., 1999. "On the Damage Survivability of Ro-Ro Ships Investigated by Motion Simulation in a Seaway", Schiffstechnik – Ship Technology Research, Vol. 46, pp. 192-207.

Cho, S. K., Hong, S. Y., Kim, Y. H., and Lee, K. J., 2005. "Investigation of dynamic characteristics of the flooding water of the damaged compartment of an ITTC RORO Passenger Ship", Proceedings of the 8th International Ship Stability Workshop, Istanbul, Turkey, 6-7 October 2005.

Clift, R., Grace, J.R., and Weber, M.E., 1978. Bubbles, Drops, and Particles, Academic Press Inc., New York, p.205.

FLOODSTAND Project Consortium, 2011. WP2 - Flooding Progression Modelling, Deliverable No. D2.3, D2.4a, D2.4b, FLOODSTAND Project Consortium, EU.

Ikeda, Y., Ishida, S., Katayama, T., and Takeuchi, Y., 2004. "Experimental and Numerical Studies on Roll Motion of a Damaged Large Passenger Ship in Intermediate Stages of Flooding", Proceedings of the 7th International Ship Stability Workshop, Shanghai, China, 1-3 November 2004, pp. 42-46.

ITTC, 2011. "Final Report and Recommendations to the 26th ITTC, The Specialist Committee on Stability in Waves", Proceedings of 26th ITTC, Rio de Janeiro, Brazil, 28 August - 3 September 2011, pp.523-560.

KRISO, 2014. Analysis of the cause of a sinking accident of MV Sewol (Simulation of Maneuvering, Flooding, and Sinking), Report No. UCPGS2750-10546-6. KRISO, Korea, pp.114-129. (in Korean)

Lamb, H., 1945. Hydrodynamics, Dover Publications, Inc., New York. (republication of the 6th(1932) edition by Cambridge University Press), p.164.

Lee, G. J., 2010a. "Simplified Modelling of Floodwater Dynamics", Proceedings of the Annual Autumn Meeting, SNAK, Changwon, 21-22 October 2010, pp.969-974. (in Korean)

Lee, G. J., 2010b. "Flow through Openings for Flooding Calculation", Proceedings of the Annual Autumn Meeting, SNAK, Changwon, 21-22 October 2010, pp.979-990. (in Korean)

Lee, G. J., 2014. "A Study on the Dynamic Orifice Equation for the Flooding Simulation of a Ship", Journal of Ships & Ocean Engineering, vol. 55., pp.17-27. (in Korean)

Lee, G. J., 2015. "Dynamic orifice flow model and compartment models for flooding simulation of a damaged ship", Ocean Engineering (submitted).

Papanikolaou, A., Zaraphonitis, G., Spanos, D., Boulougouris, E., and Eliopoulou, E., 2000. "Investigation into the Capsizing of Damaged Ro-Ro Passenger Ships in Waves", Proceedings of the 7th International Conference on Stability of Ships and Ocean Vehicles, Launceston, Tasmania, Australia, 7-11. February 2000, pp. 351-362.

Ruponen, P., 2007. Progressive Flooding of a

Damaged Passenger Ship, Doctoral Dissertation, Helsinki University of Technology, Finland.

Spouge, J. R., 1986. "The Technical Investigation of the Sinking of the Ro-Ro Ferry European Gateway", Transactions of Royal Institute of Naval Architects, RINA, Vol. 128, pp. 49-72.

Sen, P. and Konstantinidis, C., 1987. "A Time Simulation Approach to the Assessment of Damage Survivability of Ro/Ro Cargo Ships", Transactions of Society of Naval Architects and Marine Engineers, SNAME, Vol. 95, pp. 337-355

van't Veer, R. and de Kat, O., 2000. "Experimental and Numerical Investigation on Progressive Flooding in Complex Compartment Geometries", Proceedings of the 7th International Conference on Stability of Ships and Ocean Vehicles, Launceston, Tasmania, Australia, 7-11 February 2000, pp. 305-321.

van't Veer, R., de Kat, O., and Cojeen, P., 2002. "Large Passenger Ship Safety: Time to Sink", Proceedings of the 6th International Ship Stability Workshop, New York, U.S.A, 13-16 October, 2002.

van't Veer, R., Peters, W., Rimpelä, A-L., and de Kat, J., 2004. "Exploring the Influence of Different Arrangements of Semi-Watertight Spaces on Survivability of a Damaged Large Passenger Ship", Proceedings of the 7th International Ship Stability Workshop, Shanghai, China, 1-3 November 2004.

Vassalos, D., Jasionowski, A., and Guerin, L., 2005. "Passenger Ship Safety – Science Paving the Way", Proceedings of the 8th International Ship Stability Workshop, Istanbul, Turkey, 6-7 October 2005.

White, F. M., 1979. Fluid Mechanics, McGraw-Hill, New York, pp. 159-163, Chapter 6,10.

Woodburn, P., Gallagher, P., and Letizia, L., 2002. "Fundamentals of Damage Ship Survivability", Transactions of Royal Institute of Naval Architects, RINA, Vol. 144, pp.143-163.

APPENDIX A. Square Root Instability

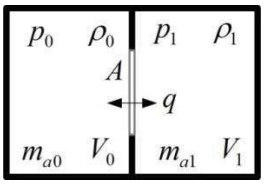

Fig. A-1 Arrangement of the sample problem

The hydraulic orifice equation was originally for steady state, let us see what happens if we apply it for an unsteady case. Here, the point of focus is the fact that the flow velocity is represented using the square root of the pressure difference. Consider the situation in Fig. A-1, in which both sides are filled with air, and there is an opening between them. The final state is the one in which the pressures on both sides are the same, so the pressure difference is zero.

Let us formulate the above situation. The flow could be represented as

$$q = sgn(\Delta p)\rho A\sqrt{\frac{2|\Delta p|}{\rho}} = sgn(\Delta p)A\sqrt{2\rho}\sqrt{|\Delta p|} \quad \text{(A-1)}$$

The mass would change to

$$\dot{m}_{a0} = -q \qquad \dot{m}_{a1} = q \quad \text{(A-2)}$$

The density at each compartment could be represented by

$$\rho_0 = m_{a0}/V_0 \qquad \rho_1 = m_{a1}/V_1 \quad \text{(A-3)}$$

The pressure in each compartment can be determined under the assumption of iso-entropic process of air. (γ is the specific heat, 7/5 for an iso-entropic process, and 1 for an iso-thermal process)

$$p_0 = k_a\rho_0^\gamma - p_{atm} = k_a\left(\frac{m_{a0}}{V_0}\right)^\gamma - p_{atm}$$
$$p_1 = k_a\rho_1^\gamma - p_{atm} = k_a\left(\frac{m_{a1}}{V_1}\right)^\gamma - p_{atm} \quad \text{(A-4)}$$
where $k_a = p_{atm}/\rho_{atm}^\gamma$.

Take the time differentiation of the above equations,

$$\dot{p_0} = \gamma\frac{k_a}{V_0}(m_{a0})^{\gamma-1}\dot{m}_{a0} = -\gamma\frac{k_a}{V_0}(m_{a0})^{\gamma-1}q$$
$$\dot{p_1} = \gamma\frac{k_a}{V_1}(m_{a1})^{\gamma-1}\dot{m}_{a1} = \gamma\frac{k_a}{V_1}(m_{a1})^{\gamma-1}q \quad \text{(A-5)}$$

Here, we assume the same volume of compartments (i.e., $V_0 = V_1$). If the pressures are the same initially, then air masses in both compartments are the same initially. Assume the change of air masses is small, and the mass could be assumed as constant m_a for the last expression of Equation A-5. If the flow through an opening increases the pressure of one compartment, the pressure of the other compartment goes down, so that $p_1 = -p_0$.

$$\dot{p_0} = -\gamma\frac{k_a}{V}(m_a)^{\gamma-1}sgn(p_0)A\sqrt{2\rho}\sqrt{2|p_0|} \quad \text{(A-6)}$$

The atmospheric pressure is large enough so that the density is nearly constant, so Equation A-6 can be rewritten as

$$\dot{p_0} = -\gamma\frac{k_a}{V}(m_a)^{\gamma-1}sgn(p_0)2A\sqrt{\rho_{atm}}\sqrt{|p_0|}$$
$$= -2\gamma\frac{A}{V^{2-\gamma}}\frac{p_{atm}}{\sqrt{\rho_{atm}}}sgn(p_0)\sqrt{|p_0|} \quad \text{(A-7)}$$

Let us rewrite this into a simpler form.

$$\dot{p} = -Ksgn(p_0)\sqrt{|p_0|} \quad \text{(A-8)}$$
where $K = 2\gamma\frac{A}{V^{2-\gamma}}\frac{p_{atm}}{\sqrt{\rho_{atm}}}$

The value of K is very large. One solution of the above equation is $p = 0$, which is what we want. Let us examine the numerical solution, using the Euler method,

$$p^{n+1} = p^n - Ksgn(p)\sqrt{|p^n|}\Delta t \quad \text{(A-9)}$$

We know the pressure would bounce around zero, because of the large value of K. Let us seek the amplitude of oscillation p^*.

$$-p^* = p^* - K\sqrt{p^*}\Delta t \;\rightarrow\; 2p^* = K\sqrt{p^*}\Delta t$$
$$\therefore\; p^* = 0 \;\; or \; p^* = \frac{(K\Delta t)^2}{4} \quad \text{(A-10)}$$

The oscillating solution is as follows.

$$p^n = (-1)^n(K\Delta t)^2/4 \quad \text{(A-11)}$$

No matter what the absolute value of the pressure was initially, the amplitude of pressure oscillation converges to p^*. That is a type of self-sustained oscillation (or self-excited). Even though we use the predictor-corrector, or Runge-Kutta method, the pressure will not go to zero, and does not oscillate as in Fig. A-2.

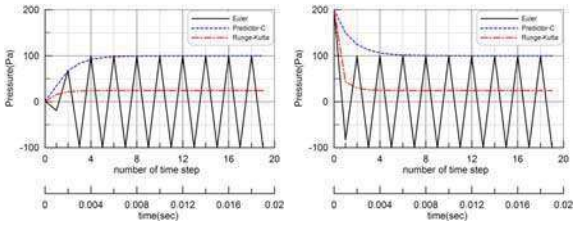

Fig. A-2 Numerical solution of the air pressure revealing the square root instability. (K=20000, Δt=0.001, p^*=100)

The above figure shows that even if the initial value is infinitesimally small (not zero) or larger than p^*, the result of the Euler method oscillates back and forth around zero and the amplitude grows to p^*. However, the results of the predictor-corrector do not oscillate and go to the value of p^*. Even for the Runge-Kutta method, it goes to about 1/4 p^*, not zero. This is numerically unstable. Because the predictor-corrector and Runge-Kutta methods give non-zero solutions, they are dangerous compared with the Euler method. The result of the Euler method gives values whose average is zero. We expected the solution to go to zero, but it does not, so this phenomenon can be called numerical instability.

Let us investigate the value of K,

$$K = 2\gamma \frac{A}{V^{2-\gamma}} \frac{p_{atm}}{\sqrt{\rho_{atm}}}$$

Substitute the real values except A and V(ρ_{atm}=1.26 , p_{atm} ≅100,000)

$$K = 178{,}174 \times \gamma \frac{A}{V^{2-\gamma}} = 356{,}348 \times \frac{A}{V^{0.6}} \quad \text{(A-12)}$$

In order to maintain p^* as less than 100 Pa (i.e., 1/1000 of atmospheric pressure; this would be accepted as a negligible amount in the engineering sense) the time interval of simulation should be the following value.

$$\Delta t^* = 20/K = 5.6 \times 10^{-6} \frac{V^{0.6}}{A}$$

For example, a passenger ship has many rooms in which the dimensions are about 4m(depth), 3m(width), and 2.5m(height), for which the area of door is 2m^2, and for that room Δt=0.00022. This is not practical. For a larger compartment of 10m x 10m x 5m, with a 2m^2 door, the time interval should be Δt =0.001. Therefore, this is impractical because of the numerical instability of the square root.